Journal of Academia Vol. 14, Issue 1 (2026) 72 – 81

SYNTHESIS AND OPTIMIZATION OF RICE BRAN AND MUSSEL SHELL POWDER BIOCHAR FOR HEAVY METAL ADSORPTION IN WATER

Zhixin Liu[1,2], Faeiza Buyong[1*], Chia Chay Tay[1], Yuling Zhu[1,2], Jinqi Han[2], Chengjue Bi[2], Qi Bian[2,3]

[1]*Faculty of Applied Sciences, Universiti Teknologi MARA, Shah Alam, Selangor, 40450, Malaysia*
[2]*School of Environmental and Sciences, Shaoxing University, Shaoxing 312000, China*
[3]*Shaoxing Zeyuan Technology Co., Ltd., Shaoxing, 312000, China*

[*]*Corresponding author: faeiza@uitm.edu.my*

Abstract

Heavy metal pollution poses a serious threat to human health and environmental safety. Therefore, researchers are highly concerned about finding low-cost and safe biochar modification solutions. This study used rice bran and mussel shell powder as raw materials to synthesize calcium phytate biochar. The synthesis conditions were optimized based on the characterization and adsorption experiment results. The results showed that the raw biochar synthesized by the hydrothermal carbonization at 200 °C (H-200) had the largest surface area of 51.09 $m^2 \cdot g^{-1}$. The biochar synthesized from H-200 at different ratios of phytic acid and mussel shell powder became rough in surface and possessed rich mesoporous structures and key functional groups such as C-O, -OH, and C=O that enhanced adsorption. The sample 1P-1.5 exhibited the best adsorption effect 60.1 ± 0.1 % (n=3) of Cd^{2+} and 100.0 ± 0.2 % (n=3) of Pb^{2+}, indicating potential for further applied research.

Keywords: Heavy metal treatment, calcium phytate biochar, rice bran, mussel shell powder.

Article History:- Received: 10 September 2025; Revised: 21 October 2025; Accepted: 15 December 2026; Published: 30 April 2026

Introduction

Heavy metal pollution is a serious environmental issue arising from modern industrial development, posing a threat to human health and sustainable development (Ye et al., 2024; Zeng et al., 2025). The biochar produced from biomass has been proven to be an excellent adsorbent. It has been confirmed to have a well-developed microporous structure, a high specific surface area, and abundant functional groups, which can remove heavy metal ions from water bodies (Aziz et al., 2024; Yameen et al., 2024). This is a sustainable and win-win strategy that can achieve environmental restoration during the process of promoting the recycling of biomass waste (Oral et al., 2024; Wang et al., 2024). Both the materials' feedstock type and pyrolysis temperature impacted surface morphology and remediation performance, thus reduced the reliable application of biochar in studies (Ye et al., 2024). To promote the application of biochar in environmental heavy metal remediation, researchers have modified biochar through various methods such as acid-base modification, nano-material loading/composite and chemicals or metals loading (Nosratabad et al., 2024; Shi et al., 2024). Although researchers have conducted numerous laboratory studies, they are still constrained by issues such as complex raw materials, high production costs, secondary pollution and difficult for practical application (Nguyen et al., 2023). Therefore, developing efficient, low-cost, and low-secondary-pollution modified biochar is an urgent focus.

This study utilizes rice bran and mussel shell powder as raw materials from agricultural waste to develop a calcium-based material loaded with phosphoric acid-activated biochar. The synthesis conditions were optimized, and the physicochemical properties of the material were analyzed (Anand et al., 2023). The results showed that the new biochar had a high adsorption capacity, could control the problem of heavy metal pollution, and provided a new method for the secondary resource utilization of biological waste. Therefore, this study aims to: (1) synthesize phytic-acid-calcium-modified biochar from rice bran and

mussel-shell wastes via hydrothermal carbonization and optimize the conditions; (2) systematically optimize the loading ratio of phytic acid and mussel-shell powder to maximize the removal efficiency of Cadmium (II) (Cd^{2+}) and Lead (II) (Pb^{2+}) by experiments conducted under controlled pH conditions; and (3) characterize the physico-chemical properties of modified modified calcium phytate biochar 1P-1.5. The findings are not only expected to provide a green, low-cost, and scalable remediation strategy for heavy-metal-contaminated waters but also promote waste to resource through the sustainable utilization of agricultural and fishery wastes.

Methods

Material pre-treatment

The rice bran was crushed and passed through a 60 mesh sieve. A 20 g of rice bran was weighed and placed in a 250 mL Erlenmeyer flask. Then, 160 mL of 1% (w/w) hydrochloric acid was added, and extracted using an ultrasonic bath for 8 minutes, at 40 °C, and centrifuged. Then, the supernatant was extracted using the same method for the second time. Supernatants obtained from the two extractions were mixed. The anion exchange resin (717) and the cation exchange resin (723) were successively used for filtering the obtained solution. After that, under reduced pressure conditions, vacuum distillation was employed to concentrate the solution to a 50 % phytic acid solution and the concentration of phytic acid was determined by the zinc sulfate titration method (Zhang & Bai, 2014). The moss on the pearl mussel shells was removed, and the shells were dried at 60 °C. Samples were then crushed with a hammer, ground in a crusher, and finally sieved through a 120-mesh screen. The particle size distribution of the obtained powder is about 160-mesh to 120-mesh.

Optimization of hydrothermal and pyrolysis methods

Two treatment methods were used in the synthesis of raw biochar, namely hydrothermal and pyrolysis (Figure 1) (Juturu et al., 2024; Sharma et al., 2024; Wei et al., 2025). For the hydrothermal method, 20 g of acid-impregnated rice bran filter residue and 60 mL of ultrapure water were placed in a 100 mL reactor. Samples were reacted in an oven at 150 °C, 200 °C, and 250 °C for 2h, respectively. After the reactor had cooled completely, the mixture was removed, filtered, and dried. The obtained samples were labelled as H-150, H-200, and H-250, respectively. For pyrolysis, 40 g of acid-impregnated rice bran filter residue was weighed, placed in a crucible, heated at 300, 500 or 700 °C for 4 h, and removed after cooling. The samples obtained were known as P-300, P-500, and P-700, respectively. The 6 groups of synthesized biochars were crushed and passed through 120 mesh sieves. The samples were placed in labelled polyethylene bags, vacuum-sealed, and stored for further use. Characterization of SEM and BET surface area was conducted to understand the surface morphology and porosity of samples for the selection of biochar for modification.

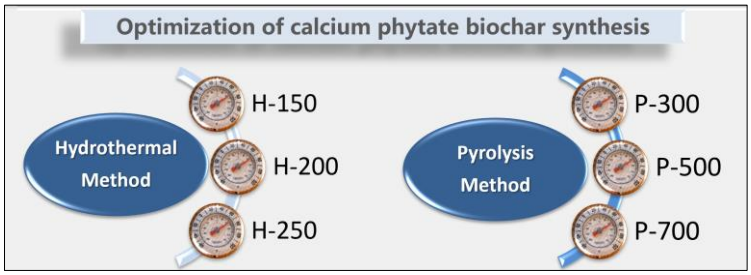

Figure 1. Temperature variation optimization of raw biochars using hydrothermal and pyrolysis methods

Calcium phytate Modification and optimization the conditions by Adsorption Study

With 50% phytic acid solution, 50 mL of 1%, 5%, and 10% phytic acid solution were prepared. A 2 g of selected biochar was weighed and added into samples, respectively. Samples were stirred with a magnetic stirrer for 2 h. Subsequently, 0.5, 1.0, 1.5, and 2.0 g of mussel shell powder were added to each sample, and the mixtures were stirred for a 8 h before the pH was measured. After three times centrifuged and washed with water, the samples were freeze-dried and labeled 1P-(0.5, 1, 1.5, 2), 5P-(0.5, 1, 1.5, 2) and 10P-(0.5, 1, 1.5, 2), respectively. Upon drying and cooling, the samples were vacuum sealed in polyethylene bags and stored in a desiccator

.
The influence of modification protocol and solution pH 2–6 (adjusted by 0.1mol·L^{-1} HCl and 0.1mol·L^{-1} NaOH) on the removal of Cd^{2+} and Pb^{2+} was investigated to identify the optimum biochar. Briefly, 100 mL aliquots of 25 mg·L^{-1} Cd^{2+} and Pb^{2+} solutions were adjusted to pH 2–6 and transferred into 250 mL Erlenmeyer flasks. A 5 mL aliquot was immediately withdrawn, filtered (0.45 µm), and labelled 0 h to determine initial concentrations. Subsequently, 0.1 g of each biochar (samples 1P-1 to 10P-2) was added, and the suspensions were shaken at 30 °C and 100 rpm for 2 h. After equilibration, another 5 mL aliquot was filtered and labelled 2 h. Residual Cd^{2+} and Pb^{2+} concentrations in both 0 h and 2 h samples were measured by flame atomic absorption spectrophotometry.
After adsorption, the content of Cd^{2+} or Pb^{2+} in the filtrate was determined, i.e., C_{eq} (3 parallel sets, i.e., 3 repetitions), using equation (1):

$$q = \frac{V \times C_0 \times C_{eq})}{m} \quad (1)$$

The adsorption capacity q was calculated according to the formula, where V is the solution volume of the sample, m is the mass of the adsorbent added. Meanwhile, the removal percentage was calculated by equation (2):

$$RP = \frac{C_0 \times C_{eq}}{C_0} \times 100\% \quad (2)$$

The process was conducted as shown in Figure 2.

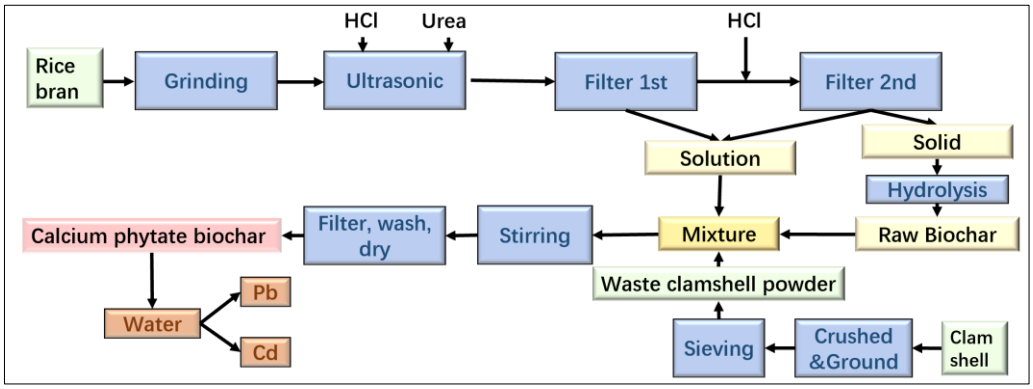

Figure 2. Flowchart of the synthesis and modification process

Characterization of the chosen optimized synthesized biochar
The synthesized biochars were systematically compared for surface morphology, elemental composition, and functional groups. Micro-morphological features of the biochars before and after modification were acquired by scanning electron microscopy (SEM). Specific surface area and porosity properties were quantified by Brunauer–Emmett–Teller (BET) surface area and pore-size analysis. Surface functional groups of the biochars before and after modification were identified by Fourier-transform infrared spectroscopy (FTIR), and the key chemical bonds of the calcium phytate loading sample biochar was assessed by X-ray photoelectron spectroscopy (XPS) (Ravindiran et al., 2024).

Result and Discussion

SEM analysis of biochars synthesized with different methods and temperatures
Figure 3 shows the SEM micrographs of H-150, H-200 and H-250 samples that were synthesized by hydrothermal method and the P-300, P-500 and P-700 were synthesized by the pyrolysis method before modification process. SEM result indicates that H-150 showed a layered structure, and the surface structure still resembles that of rice bran, whereas the H-200 and H-250 displayed regular spherical particles, the heterogeneity of spherical particle size was the typical microstructure of the materials. In

contrast, the P-300, P-500 and P-700 samples, prepared by the pyrolysis method, exhibited irregular porous surface structure. The surface morphology of P-500 and P-700 samples changed significantly, showing an irregular fragments structure due to modification. This is consistent with previously reported results (Cheng & Li, 2018). Hence, the layered and microstructure of spherical particles biochars by hydrothermal method was selected for further BET analysis.

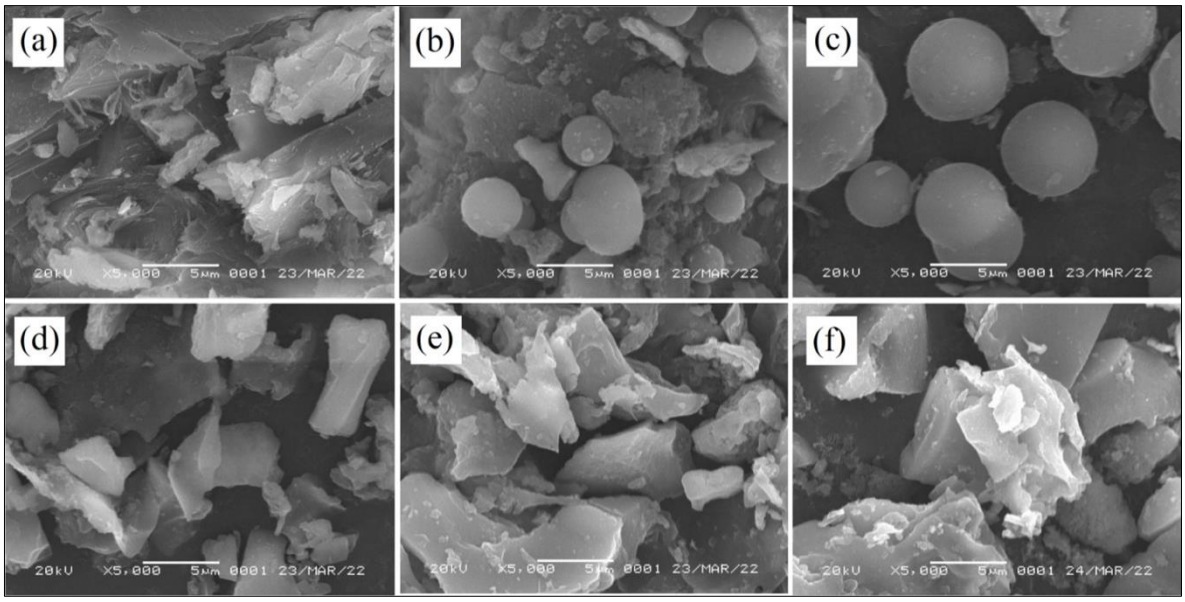

Figure 3. SEM images of H-150(a), H-200(b), H-250(c), P-300(d), P-500(e), P-700(f)

BET analysis of biochars synthesized with different methods and temperatures

The Brunauer–Emmett–Teller (BET) analysis results for the specific surface area and pore size of the synthesized biochars by hydrothermal method is presented in Table 1. Among the six samples, H-200, synthesized via hydrothermal carbonization at 200 °C, exhibited the largest specific surface area of 51.09 $m^2 \cdot g^{-1}$. This may due to the optimal carbonization conditions at this temperature, which facilitated the formation of a porous structure. In contrast, samples synthesized at lower (H-150) or higher (H-250) temperatures displayed smaller surface areas. This suggests that the hydrothermal carbonization method at 200 °C is more effective in producing biochar with a larger specific surface area, which is crucial for adsorption applications as it provides more sites for heavy metal ions to bind. (Elnour et al., 2019) supported the findings that the specific surface area of biochar increased with temperature. Following the selection of H-200 as the base material, calcium phytate was loaded onto the biochar for modification.

Table 1. Biochar specific surface area and pore size data

Sample	BET surface area ($m^2 \cdot g^{-1}$)	Pore size (nm)
H-150	45.12	153.52
H-200	51.09	139.43
H-250	44.24	163.53
P-300	42.43	163.52
P-500	43.42	164.03
P-700	40.87	165.24

Adsorption Study of Synthesized modified biochars

Table 2 – 4 show the capability and removal percentage of Cd^{2+} and Pb^{2+} adsorption by the synthesized biochars. The lowest residual concentration for Cd^{2+} occurred at pH 4, while for Pb^{2+}, it occurred at pH 6. For Cd^{2+}, the lowest concentration is 10.12 $mg \cdot L^{-1}$ and the adsorption efficiency is 60.1 ± 0.1 % (n=3). For Pb^{2+}, the lowest concentration is 0.005 $mg \cdot L^{-1}$, the adsorption efficiency is 100.0 ± 0.2 % (n=3).

This is because when the pH value is low, the solution is highly acidic and the content of H^+ in the solution is high. It antagonizes the positively charged Cd^{2+} and Pb^{2+}, thereby reducing the occurrence of the complex reaction of these two heavy metal ions. Since Pb^{2+} starts to precipitate at a pH 6 (He et al., 2019), the experimental results under pH 6 deviate from the actual adsorption results. Therefore, pH 5 is chosen for further study. From the results, it can be observed that 1P-1.5 achieved the best adsorption effect among all the samples. This was attributed to the appropriate ratio of phytic acid concentration and the calcium ions that can be used for ion exchange, working together for the adsorption of heavy metal. Through one-way analysis of variance, it was found that for Cd, the change in pH value had no significant effect ($p = 0.3715 > 0.05$), while for Pb, the change in pH value had a significant effect ($p = 0.0001 < 0.01$).

Table 2. The capability of Cd^{2+} adsorption by the synthesized biochar

Concentration	pH 2 ($mg \cdot L^{-1}$)	pH 3 ($mg \cdot L^{-1}$)	pH 4 ($mg \cdot L^{-1}$)	pH 5 ($mg \cdot L^{-1}$)	pH 6 ($mg \cdot L^{-1}$)
Blank	25.165	24.69	25.335	25.69	25.335
1P-1	25.79	10.445	16.255	17.635	18.205
1P-1.5	25.625	12.525	**10.12**	16.775	17.385
1P-2	24.555	19.265	13.745	17.48	18.155
5P-0.5	25.535	25.605	25.945	25.595	24.38
5P-1	25.79	25.535	25.365	25.855	24.865
5P-1.5	24.74	25.235	25.065	24.605	24.495
5P-2	24.405	21.48	20.425	20.815	21.195
10P-0.5	25.195	26.13	25.81	25.275	24.12
10P-1	23.925	25.425	25.635	24.545	24.995
10P-1.5	25.385	25.165	25.385	24.73	24.555
10P-2	25.115	24.945	25.665	25.065	24.835

Table 3. The capability of Pb^{2+} adsorption by the synthesized biochar

Concentration	pH 2 ($mg \cdot L^{-1}$)	pH 3 ($mg \cdot L^{-1}$)	pH 4 ($mg \cdot L^{-1}$)	pH 5 ($mg \cdot L^{-1}$)	pH 6 ($mg \cdot L^{-1}$)
Blank	26.14	27.375	27.09	26.385	25.54
1P-1	23.675	24.125	16.035	13.63	0.565
1P-1.5	20.33	15.325	11.275	0.205	**0.005**
1P-2	17.305	16.42	12.72	1.495	0.045
5P-0.5	25.19	24.105	21.77	18.355	18.185
5P-1	25.655	24.135	21.735	20.82	19.905
5P-1.5	26.005	21.985	19.52	16.49	15.465
5P-2	26.03	22.005	19.78	16.85	16.34
10P-0.5	25.295	21.525	17.895	16.345	16.455
10P-1	25.72	22.905	20.96	19.59	18.255
10P-1.5	25.575	21.915	18.745	16.345	16.56
10P-2	25.26	24.835	22.795	19.27	17.545

Table 4. The capability and removal percentage of Cd^{2+} and Pb^{2+} adsorption by the synthesized biochar

	q_e ($mg \cdot g^{-1}$)	*RP* (%)
Cd^{2+} (pH 4, 25 °C, n=3)	15.505	60.1 ± 0.1 %
Pb^{2+} (pH 6, 25 °C, n=3)	20.325	100.0 ± 0.2 %

SEM analysis of H-200 and 1P-1.5

The SEM analysis of H-200, and 1P-1.5 is shown in Figure 4. The modified calcium phytate biochar 1P-1.5 displayed a more layered structure with surface corrosion, transitioning from smooth to rough compared to H-200. This morphological change is indicative of an increased specific surface area.

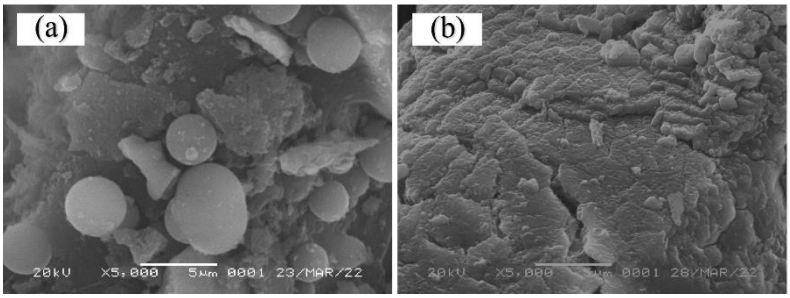

Figure 4. SEM images of (a) H-200, and (b) 1P-1.5.

Porosity analysis of H-200 and 1P-1.5

The BET analysis results for the H-200 and 1P-1.5 are shown in Table 5, further supporting the SEM findings. The modified biochar 1P-1.5 exhibited the larger specific surface area of 73.04 $m^2 \cdot g^{-1}$, but the lower pore size at 137.38 nm than the H-200. The increase in specific surface area after modification can be attributed to the introduction of calcium phytate and mussel shell powder, which likely created additional pores and functional groups on the biochar surface, thereby enhancing its adsorption capacity. In summary, the BET analysis demonstrated that the modification process significantly improved the specific surface area of the biochar, with 1P-1.5 showing the most promising characteristics for heavy metal adsorption. These results agreed with previous studies where biochar modification led to enhanced surface properties and improved adsorption performance (Elnour et al., 2019).

Table 5. Specific surface area and pore size data of H-200 and 1P-1.5

Sample	BET surface area ($m^2 \cdot g^{-1}$)	Pore size (nm)
H-200	51.09	139.43
1P-1.5	73.04	137.38

Fourier Transform Infrared Spectroscopy (FTIR) analysis of H-200 and 1P-1.5

FTIR spectra of raw biochar H-200 and calcium-phytate biochar 1P-1.5 are shown in Figure 5. Compared with the 1P-1.5, the infrared spectra of biochar before and after modification were basically the same, with similar peak shapes, indicating that its own chemical structure did not change significantly before and after modification, and all contained three main functional groups: the broadband around 1100-1150 cm^{-1} corresponded to the tensile vibration of C-OH. The broadband around 1620-1680 cm^{-1} corresponded to the tensile vibration of C=C; The broadband around 3400-3460 cm^{-1} referred to the tensile vibration of -OH. Compared with the unmodified biochar, the diffraction peak intensity of the modified calcium phytate biochar 1P-1.5 was reduced, which may be due to the loss of some crystals during the pickling process, or the destruction of some functional groups caused by the addition of activators. In order to further determine the group type, XPS was used to characterize the O1s orbital of the material.

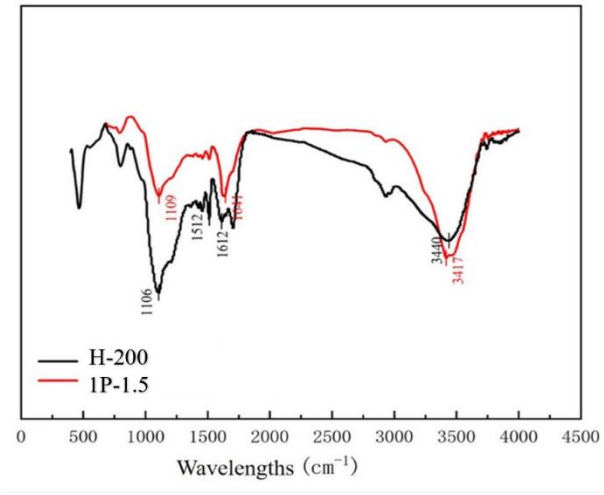

Figure 5. FTIR spectra of raw biochar H-200 and calcium phytate biochar 1P-1.5

XPS analysis of 1P-1.5

Figure 6 shows the XPS full spectrum and the O1s characteristic peaks of calcium phytate biochar 1P-1.5 analysis by Advantage 5.9931. The XPS analysis revealed that 1P-1.5 simultaneously had four components: C, O, P, and Ca. XPS analysis quantitatively characterized the surface elemental composition and chemical state of 1P-1.5. The atomic percentages of C1s, O1s, Ca2p, and P2p are 48.37%, 42.86%, 3.76%, and 5.02%, respectively. The XPS spectrum of the C1s spectrum of 1P-1.5 presented four characteristic peaks: 284.80 eV (C-C), 287.01 eV (C-O-C), 531.24 eV (C=O), and 533.09 eV (C-O). In 1P-1.5, P $2p_{3/2}$ (131.76 eV), P $2p_{1/2}$ (132.83 eV), $Ca(OH)_2$ (345.76 eV/ 349.29 eV), and $CaCO_3$ (346.39 eV/ 349.99 eV) were observed (Ani et al., 2025). The above results of XPS experiments have confirmed the loading of calcium phytate.

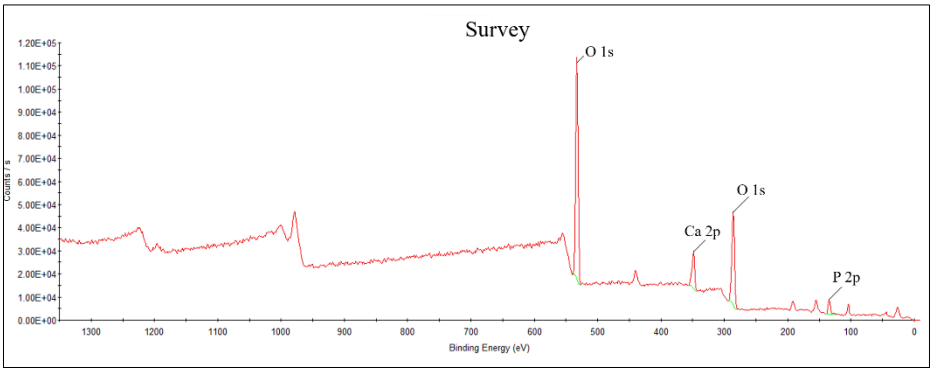

(a)

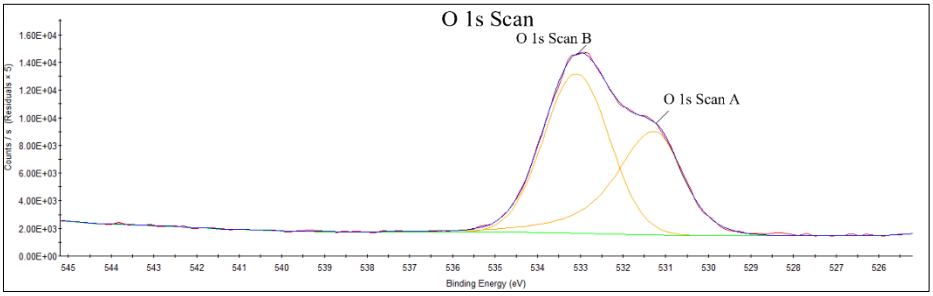

(b)

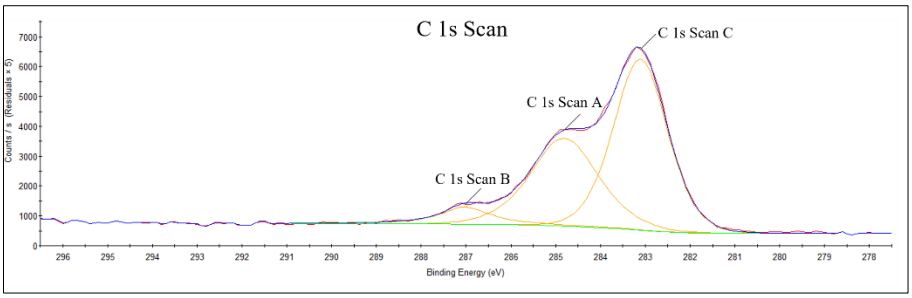

(c)

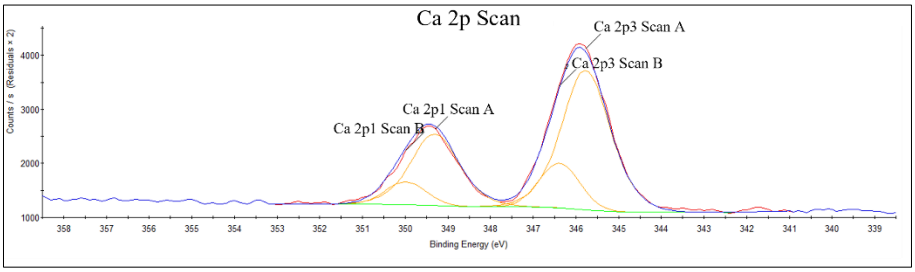

(d)

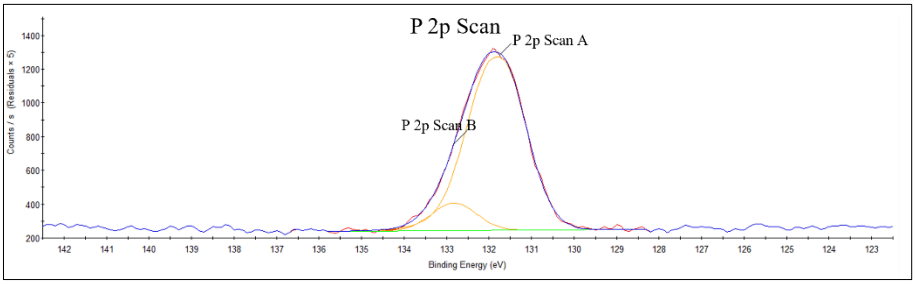

(e)

Figure 6. XPS spectra of modified calcium phytate biochar 1P-1.5. (a) Survey spectrum, (b) Oxygen, O 1s, (c) Carbon, C 1s, (d) Calcium, Ca 2p and (e) Phosphorous, P 2p

Conclusion

Heavy metal pollution in water poses a serious threat to human health and the ecological environment. In this study, agricultural waste rice bran and mussel shell powder based calcium-phytate modified biochar for heavy metals adsorption was synthesized. The synthesized biochar was characterized and tested for its adsorption capacity under different pH environments. The optimal reaction conditions and the best ratio were then determined. The experiment showed that rice bran biochar synthesized by the hydrothermal method at 200 °C has the largest specific surface area of 51.09 °C·g^{-1}, and it was used in further modification. The adsorption experiment was investigated to examine the best performance of biochars. The best biochar was 1P-1.5, as it achieved the best results in both of the heavy metal adsorption experiments at 60.06 % for Cd^{2+} and 99.98 % for Pb^{2+}. The optimal adsorption pH condition for Cd^{2+} was pH 4, while for Pb^{2+}, pH 6 was the best. After modification, the calcium phytate biochar 1P-1.5 showed a stacked pore structure, large surface area and functional groups such as C-O, -OH, and C=O. This information is vital for future research focuses on the mechanisms and the life cycle assessment to account for sustainability.

Acknowledgement/Funding

The author(s) received financial support from: International Strategic Research Partnership Research Grant between UiTM and USX (No.100-RMC 5/3/SRP INT (035/2023)), Horizontal Projects of Industry-University Cooperation by the Science and Technology Department of Zhejiang Province (No.2022330001004125).

Author Contribution

Z Liu – conceptualization, methodology, formal analysis, writing - original draft preparation, data curation. F Buyong – supervision, data curation. TC Chay – project administration, writing – review & editing. J Han – visualization, investigation, C Bi – software, validation. Q Bian – resources, funding acquisition.

Data availability

The raw data for adsorption/characterization available will be provided upon request.

Conflict of Interest

Authors declare no conflict of interest.

Declaration on the Use of Generative AI

Authors declare no generative AI used in the manuscript.

References

Anand, A., Gautam, S., & Ram, L. C. (2023). Feedstock and pyrolysis conditions affect suitability of biochar for various sustainable energy and environmental applications. *Journal of Analytical and Applied Pyrolysis*, *170*, Article 105881. https://doi.org/10.1016/j.jaap.2023.105881

Ani, P. C., Al-Abedi, H. J., Smith, J. D., & Zeitoun, Z. (2025). Biochar surface chemistry modification by blending hardwood, softwood, and refuse-derived fuel: Insights from XPS, FTIR, and zeta potential analysis. *Fuels*, *6*(3), 71. https://www.mdpi.com/2673-3994/6/3/71

Aziz, K. H. H., Mustafa, F. S., Hassan, M. A., Omer, K. M., & Hama, S. (2024). Biochar as green adsorbents for pharmaceutical pollution in aquatic environments: A review. *Desalination*, *583*, Article 117725. https://doi.org/10.1016/j.desal.2024.117725

Cheng, F., & Li, X. (2018). Preparation and application of biochar-based catalysts for biofuel production. *Catalysts*, *8*(9), 346. https://doi.org/10.3390/catal8090346

Elnour, A. Y., Alghyamah, A. A., Shaikh, H. M., Poulose, A. M., Al-Zahrani, S. M., Anis, A., & Al-Wabel, M. I. (2019). Effect of pyrolysis temperature on biochar microstructural evolution, physicochemical characteristics, and its influence on biochar/polypropylene composites. *Applied Sciences*, *9*(6), 1149. https://doi.org/https://doi.org/10.3390/app9061149

He, H., Zhu, Z., Liu, J., Zhu, Y., Yan, Q., Liu, Y., Mo, N., Xuan, H., & Wei, W. (2019). Removal of Pb^{2+} from aqueous solution by magnesium-calcium hydroxyapatite adsorbent. *Environmental Science*, *40(9)*, 4081–4090. https://doi.org/10.13227/j.hjkx.201901082

Juturu, R., Selvaraj, R., & Murty, V. R. (2024). Efficient removal of hexavalent chromium from wastewater using a novel magnetic biochar composite adsorbent. *Journal of Water Process Engineering*, *66*, Article 105908. https://doi.org/10.1016/j.jwpe.2024.105908

Nguyen, T. B., Sherpa, K., Bui, X. T., Nguyen, V., Vo, T. D. H., Ho, H. T. T., Chen, C. W., & Dong, C. D. (2023). Biochar for soil remediation: A comprehensive review of current research on pollutant removal. *Environmental Pollution*, *337*, Article 122571. https://doi.org/10.1016/j.envpol.2023.122571

Nosratabad, N. A., Yan, Q. G., Cai, Z. Y., & Wan, C. X. (2024). Exploring nanomaterial-modified biochar for environmental remediation applications. *Heliyon*, *10*(18), Article e37123. https://doi.org/10.1016/j.heliyon.2024.e37123

Oral, B., Cosgun, A., Guenay, M. E., & Yildirim, R. (2024). Machine learning-based exploration of biochar for environmental management and remediation. *Journal of Environmental Management*, *360*, Article 121162. https://doi.org/10.1016/j.jenvman.2024.121162

Ravindiran, G., Rajamanickam, S., Janardhan, G., Hayder, G., Alagumalai, A., Mahian, O., Lam, S. S., & Sonne, C. (2024). Production and modifications of biochar to engineered materials and its application for environmental

sustainability: a review. *Biochar*, *6*(1), 62. https://doi.org/10.1007/s42773-024-00350-1

Sharma, T., Hakeem, I. G., Gupta, A. B., Joshi, J., Shah, K. L., Vuppaladadiyam, A. K., & Sharma, A. (2024). Parametric influence of process conditions on thermochemical techniques for biochar production: A state-of-the-art review. *Journal of the Energy Institute*, *113*, 101559. https://doi.org/10.1016/j.joei.2024.101559

Shi, X., Yang, W. Q., Li, J., & Yao, Z. L. (2024). The application of biochar as heavy metals adsorbent: The preparation, mechanism, and perspectives. *International Journal of Environmental Research*, *18*(3), 41. https://doi.org/10.1007/s41742-024-00592-8

Wang, C. Q., Lin, X., Zhang, X. X., & Show, P. L. (2024). Research advances on production and application of algal biochar in environmental remediation. *Environmental Pollution*, *348*, 23860. https://doi.org/10.1016/j.envpol.2024.123860

Wei, T., Hong, H. Q., Zhang, H. Y., & Wu, F. J. (2025). Comparative carbonization study of pyrolyzed biomass: New insights into the structure and composition evolution of biochar. *Bioenergy Research*, *18*(1), 13. https://doi.org/10.1007/s12155-025-10819-x

Yameen, M. Z., Naqvi, S. R., Juchelkova, D., & Khan, M. N. A. (2024). Harnessing the power of functionalized biochar: Progress, challenges, and future perspectives in energy, water treatment, and environmental sustainability. *Biochar*, *6*(1), 25. https://doi.org/10.1007/s42773-024-00316-3

Ye, W. J., Li, L., Tang, Z. L., Peng, Y., Yang, P. J., Peng, X. Y., & Zhen, F. (2024). Biochar and modified magnetic biochar enhanced anaerobic digestion of swine wastewater under ammonia stress: Performance and microbial dynamics. *Journal of Environmental Chemical Engineering*, *12*(2), 111969. https://doi.org/10.1016/j.jece.2024.111969

Zeng, Y., Song, Z., Song, G., Li, S., Sun, H., Zhang, C., & Li, G. (2025). Oxidative stress and antioxidant biomarker responses in fish exposed to heavy metals: a review. *Environmental Monitoring and Assessment*, *197*(8), 892. https://doi.org/10.1007/s10661-025-14376-w

Zhang, H. W., & Bai, X. L. (2014). Optimization of extraction conditions for phytic acid from rice bran using response surface methodology and its antioxidant effects. *Journal of Food Science and Technology-Mysore*, *51*(2), 371–376. https://doi.org/10.1007/s13197-011-0521-y